International Journal for Modern Trends in Science and Technology
Volume 10, Issue 03, pages 431-437.
ISSN: 2455-3778 online
Available online at: http://www.ijmtst.com/vol10issue03.html
DOI: https://doi.org/10.46501/IJMTST1003069

Artificial Intelligence based Landsman Converter Design for Electric Vehicle with Power Factor Correction

Ardhala Bala Krishna[1], R.Vyshnavi [2], B. Ashok Kumar [2], Sd. Bazeed [2], Ch.Jagan [2], B.Arun Kumar [2]

[1]Assistant Professor, Department of Electrical and Electronics Engineering, PSCMR College of Engineering and Technology (Autonomous), Vijayawada, AP, India.
[2]Department of Electrical and Electronics Engineering, PSCMR College of Engineering and Technology (Autonomous), Vijayawada, AP, India.

To Cite this Article
Ardhala Bala Krishna, R.Vyshnavi, B. Ashok Kumar, Sd. Bazeed, Ch.Jagan, B.Arun Kumar, Artificial Intelligence based Landsman Converter Design for Electric Vehicle with Power Factor Correction, International Journal for Modern Trends in Science and Technology, 2024, 10(03), pages. 431-437.https://doi.org/10.46501/IJMTST1003069

Article Info
Received: 02 February 2024; Accepted: 26 March 2024; Published: 30 March 2024.

ABSTRACT

The rapid growth of the electric vehicle (EV) market demands innovative solutions to enhance the efficiency and sustainability of EV charging systems. This paper introduces a novel design of a Landsman converter for EV charging applications, incorporating Artificial Intelligence (AI) techniques for Power Factor Correction (PFC). The proposed AI-based control strategy optimizes the operation of the Landsman converter, ensuring high power factor, reduced harmonic distortion, and improved energy efficiency during the EV charging process. A comprehensive simulation model of the converter is developed and analyzed using MATLAB/Simulink, demonstrating the effectiveness of the AI algorithms in achieving optimal performance under varying load conditions and input voltages. The results highlight the potential of integrating AI with power electronics to advance EV charging technologies, contributing to the development of more efficient, reliable, and smart charging infrastructure.

KEYWORDS: Electric Vehicle, Landsman Converter, Power Factor Correction, Artificial Intelligence, MATLAB/Simulink, Energy Efficiency, Harmonic Distortion, Charging Infrastructure.

1. INTRODUCTION

Electric mobility contributes significantly to the creation of a sustainable and effective alternative in the transportation industry, which is important given the severe regulations on emissions, fuel efficiency, global warming challenges, and limited energy resources. In this regard, a survey based on the current situation and potential technologies for electric vehicle (EV) propulsion is offered. Comparing electric mobility to traditional petrol-and diesel-powered vehicles, there are a number of benefits. However, if the researcher wants to completely embrace transportation electrification, they must pay particular attention[1]. It is necessary to develop appropriate, efficient control mechanisms in order to integrate them with the current distribution system. Some of the strategies listed above have to do with the poor power quality issues that EV chargers have when charging battery packs.The electric vehicles are powered by the rechargeable batteries, which also provide the necessary traction force. These batteries are usually recharged using an EV charger, commonly referred to as an AC-DC converter. A boost converter up front and an isolated converter later make up the most typical design for an electric vehicle battery charger. Because the output voltage and current are controlled, the DC-DC converter's performance alone determines how well this sort of charger performs[2] -[5].Numerous interleaved and zero voltage switching (ZVS) PFC (Power Factor Correction) converter-based battery chargers have been developed to reduce the inductor size and output current ripple. ThePFC converter interleaving, however, has a large current stress cost in switches. With benefits including high power density and high efficiency, the full-bridge topology is the most popular for PFC-based EV chargers; nevertheless, the configuration of four switches makes the charger operation difficult. An LLC (Inductor-Inductor-Capacitor) resonant converter presents an attractive alternative because to its high efficiency, minimum electromagnetic interference noise, and high power density across a wide input range. Due to the growing complexity of the design and analysis of LLC converters, unidirectional or bidirectional AC-DC converters are replacing this type of topology in integrated on-board or off-board configurations [6].

2. DIODE BRIDGE RECTIFIER

In an existing system that considers AC-DC conversion as the distinguishing feature of EV battery chargers, numerous DBR (Diode Bridge Rectifier) fed unidirectional isolated single stage or two-stage converters without isolation are recognized. In this regard, the current block diagram shows the setup of a conventional single phase DBR fed unidirectional E-rickshaw battery charger. [7] –[9]. However, the conventional charger's performance does not adhere to the required power quality (PQ) standard, IEC 61000-3-2. Full-wave diode bridges at the charger's input cause a significant level of harmonic distortion (55.3%) in the input current drawn during battery charging. The result is a low source power factor. The difference between source voltage and current is also getting wider since the input current is no longer sinusoidal. Therefore, an efficient power factor correction (PFC) technique that also mitigates the negative effects of input DBR is needed for the front-end of the conventional DBR fed charger..

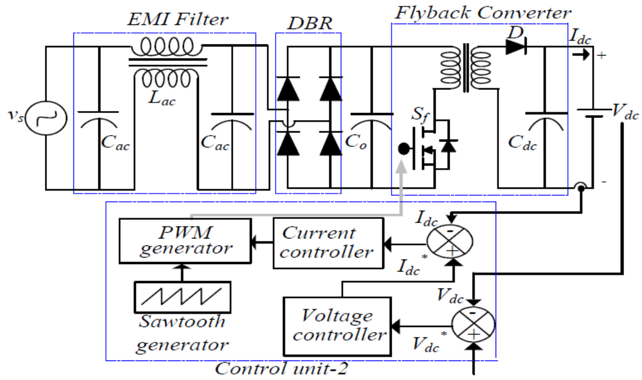

Fig 1. Diode Bridge Rectifier Configuration

3. LANDSMAN CONVERTER

By reordering the input and output side inductors, the first stage of the proposed Landsman converter differs slightly from the existing system. Due to continuous conduction (CCM) of the input inductors, the suggested change delivers the benefit of low input current ripple as well as the benefit of low output current ripple with the standard Landsman topology being maintained. To raise the power factor to unity, two parallel converters run in synchronization and in discontinuous region (DCM mode) during the respective mains voltage half cycles. Due to the employment of a single sensor at the output stage, the DCM operation has the inherent advantages of being inexpensive and simple in the circuit. The charger's intermediate DC link voltage is successfully controlled using a proportional and integral (PI) controller based on a voltage follower [17]. However, a dual loop PI controller is used to operate the flyback converter in the second stage. During the conditions of constant current and constant voltage mode charging, the battery current is regulated to correspond to 60% state of charge (SOC) to 100% SOC with the help of a straightforward PI control. As a result, the suggested EV battery charger provides the EV battery with an enhanced power quality-based charging profile. Additionally, the charger's input power quality indices were found to be within the acceptable limits of the IEC 61000-3-2 standard [20]. Due to the fact that DBR conduction losses are cut in half for each cycle, the efficiency is increased as compared to the traditional DBR fed charger.

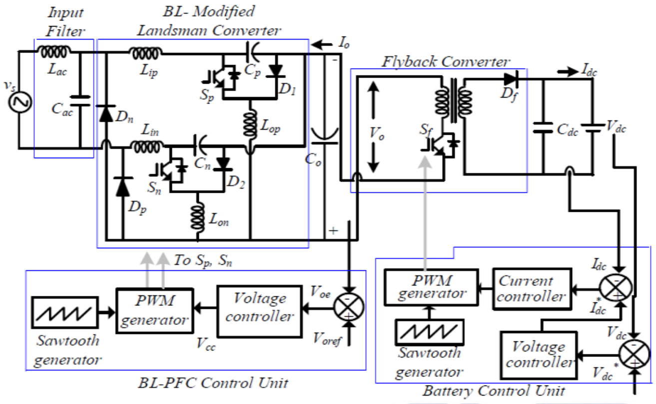

Fig 2. Landsman Converter Configuration

4. MODES OF OPERATION

Figs. 3 (a) –3 (c) Show the switching cycle and the corresponding half of the mains voltage operation of the proposed redesigned BL converter (f). The operational principle during the positive half cycle is explained in the following:

Mode P-I (t0-t1): The converter's operation starts in mode P-I during the positive half cycle of the mains voltage [10,11]. The inductor Lop begins charging through the path depicted in Fig. when the switch SP, connected in the upper line, is in the ON position. 3 (a). At this moment, the isolated converter linked to the load side causes the intermediate DC link capacitor, Co, to discharge. Due to the inductor's stored charge, the high frequency diode D1 does not have a conducting route at this time, and as a result, a reverse bias voltage is present across it.[12] – [14]

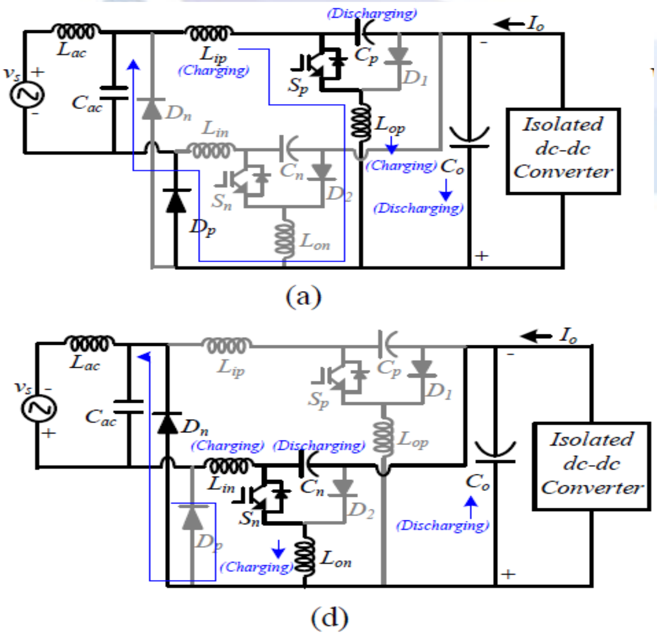

Fig: 3 (a) & (d) Mode of Operation – I

Mode P-II (t1-t2): When the gate pulse to the switch is suppressed, the high frequency diode D1 works in mode P-II. The inductor, Lop, follows the route shown in Fig. To discharge through it, use 3(b) [15, 16]. For each switching cycle, power is delivered to the flyback converter at the output and the DC link capacitor, which Co starts charging

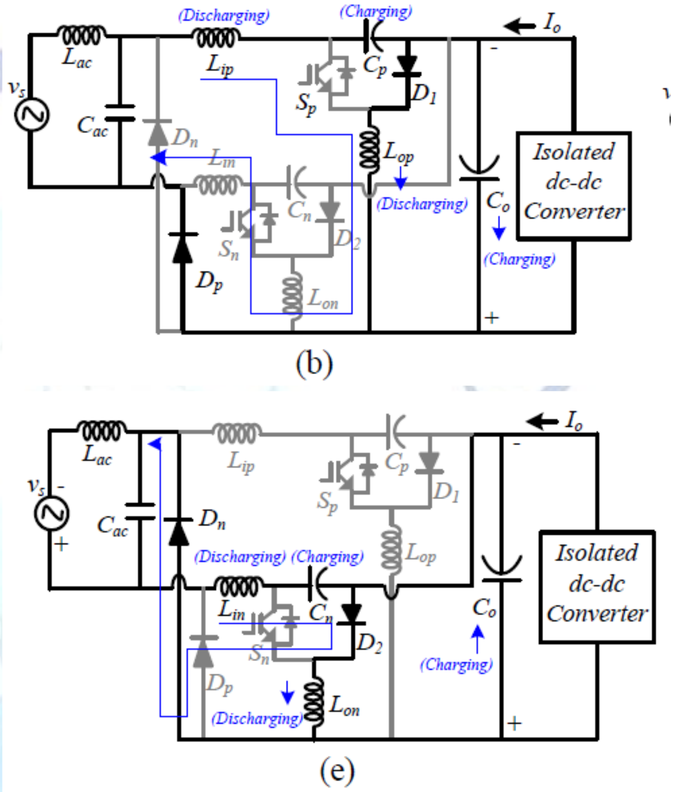

Fig: 3 (b) & (e) Mode of Operation II

Mode P-III (t2-t3): At the conclusion of the switching cycle in mode P-III operation, the stored charge in inductor Lop is totally exhausted. For the rest of the switching cycle, the inductor current discontinues [18, 19]. The intermediate DC link capacitor is responsible for supplying the output power during this time, discharging through the channel shown in Fig. 3. (c). The revised BL converter proposed switches the lower switch Sn, inductor Lon, and diode D2 in the same order throughout the negative half cycle of the mains voltage, as shown in Figs. 3(d)-(e) (f) [21, 22]. Show both the switching cycle of the suggested bridgeless Landsman converter and the switching order for the components operating in the various modes during the whole input voltage cycle

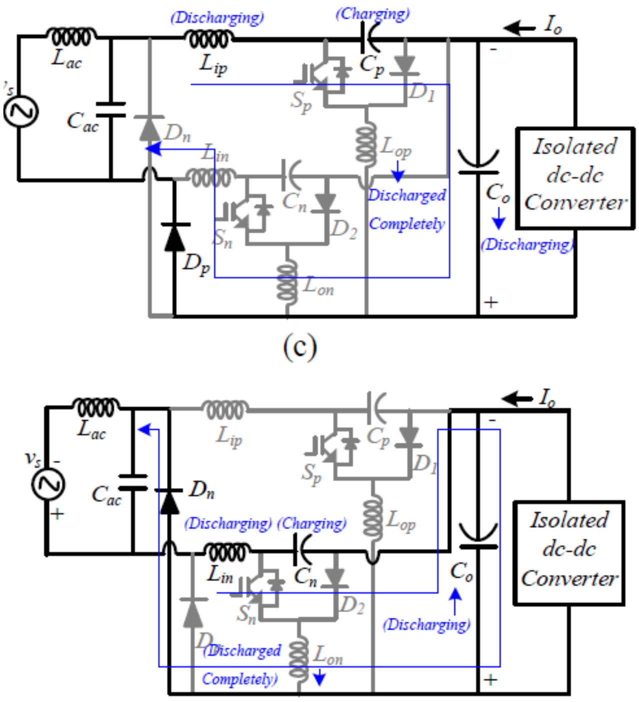

Fig: 3 (c) & (f) Mode of Operation – III

5. RBFNN based MPPT controller

This section details the RBFNN architecture, including input layer, hidden layer with radial basis function neurons, and output layer strategies. The RBFNN inputs include line voltage, line current, and load conditions, with the outputs generating PWM signals for converter control.

The RBFNN is a kind of feed forward neural network model that uses both unsupervised and supervised learning. As can be seen in Figure 4, RBFNN consists of a basic structure with three layers: an input layer, a hidden layer, and an output layer. Both the hidden and output layers employ radial basis activation functions, while the one in the hidden layer is non-linear.

The operation of RBFNN is highly influenced by the interconnection pattern, activation function and weights.

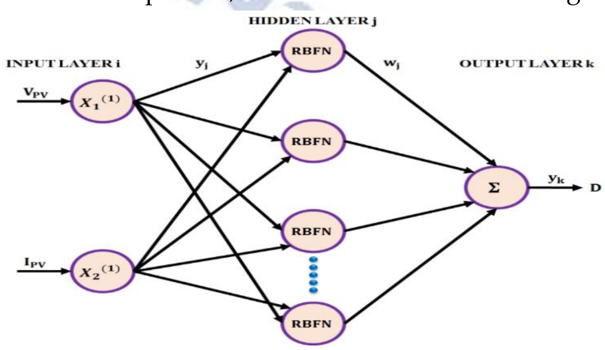

Figure 4: RBFNN based MPPT controller

The input neuron's net input and output are specified as given below.

$$x_i^{(1)}(n) = net_i^{(1)} \quad (1)$$

$$y_i^{(1)}(n) = f_i^{(1)}\left[net_i^{(1)}(n)\right] = net_i^{(1)}(n), i = 1,2 \quad (2)$$

Here, the input layer and hidden layer are denoted by the terms $x_i^{(1)}$and $y_i^{(1)}$respectively. The sum of the input layer is denoted as $net_i^{(1)}$. In the hidden layer, every node behaves like a Gaussian function. In the RBFN, the Gaussian function is used as a membership function.

$$net_j^{(2)}(n) = -(X - M_j)^T \sum_j (X - M_j) \quad (3)$$

$$y_j^{(2)}(n) = f_j^{(2)}\left[net_j^{(2)}(n)\right] exp\left[net_j^{(2)}(n)\right], j = 1,2, ... (4)$$

Here, the mean and standard deviation of the Gaussian function are specified by the terms M_j and $\sum_j$ respectively. The linear control signal (D) is generated by the output layer, which has a single node k.

$$net_k^{(3)} = \sum_j w_j y_j^{(2)} \quad (5)$$

$$y_k^{(3)} = f_k^{(3)}\left[net_k^{(3)}(n)\right] = net_k^{(3)}(n) \quad (6)$$

The connective weight matrix between both the output and hidden layer is denoted as w_j. Based on the output of the controller, the PWM generator generates PWM pulses, which adjust the duty cycle D of the Landsman converter and produce a controlled output voltage without any fluctuations.

4. RESULTS AND DISCUSSIONS

This section presents simulation results validating the effectiveness of the RBFNN control in enhancing the power factor.

Case1 : with PI control strategy

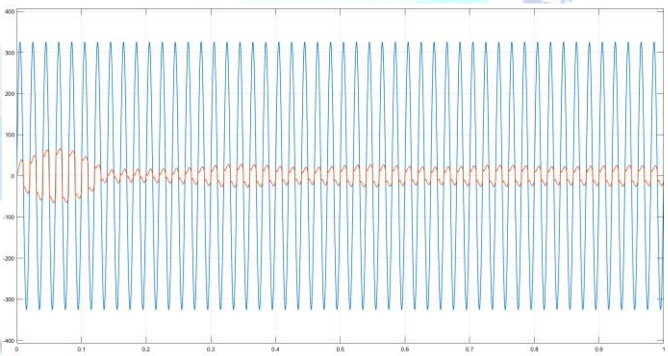

Fig: Grid Voltage and current

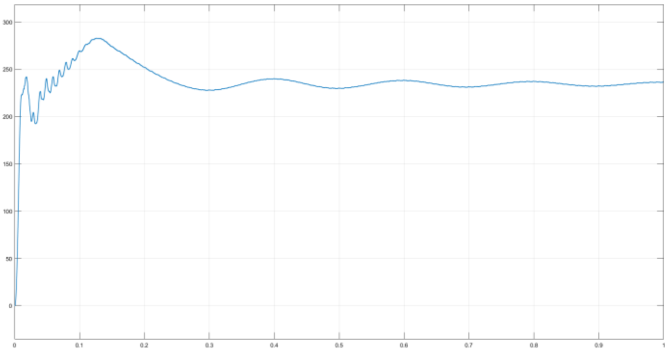

Fig: output voltage of the converter

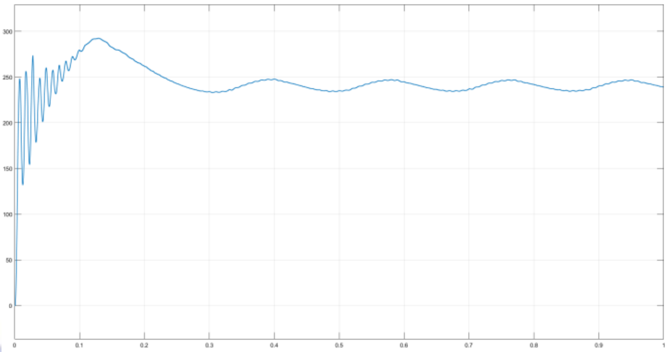

Fig: output voltage of the converter with proposed control strategy.

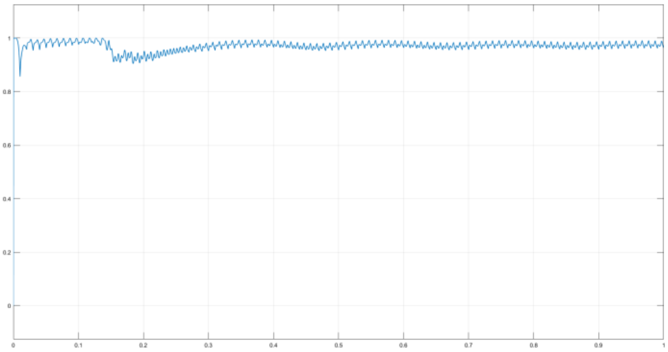

Fig: power factor of the source when fed to converter

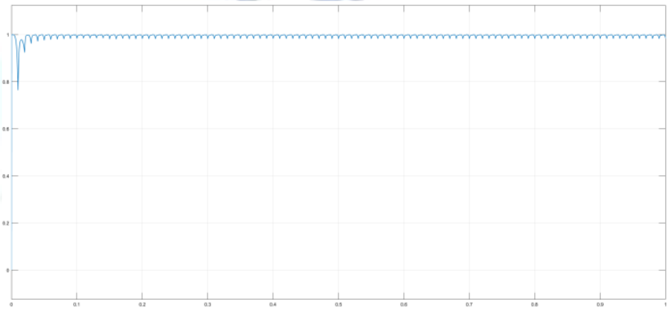

Fig: power factor of the source when fed to converter with proposed control strategy.

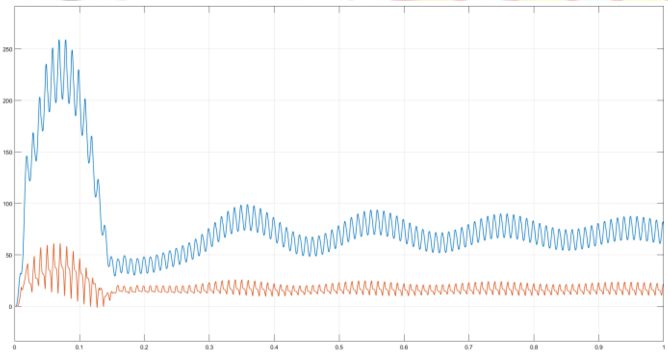

Fig: Active power and reactive power

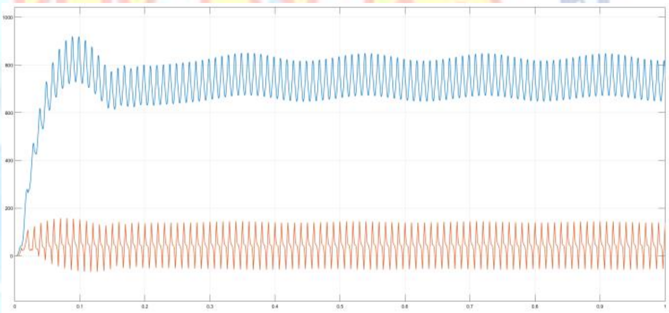

Fig: Active power and reactive power with proposed control strategy.

Case 2: with RBFNN control strategy

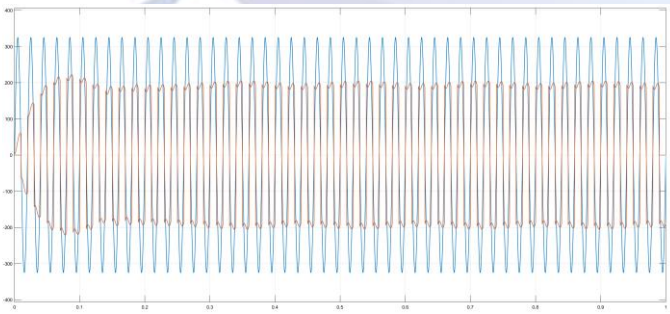

Fig: Grid Voltage and current with proposed control strategy.

Due to the fact that DBR conduction losses are cut in half for each cycle, the efficiency is increased as compared to the traditional DBR fed charger [23]. Due to the continuous conduction (CCM) of the input inductors, the proposed change has the benefit of reduced input current ripple.

5. CONCLUSION

In pursuit of optimizing electric vehicle (EV) battery charging efficiency and power factor correction, a comprehensive simulation study was conducted on a novel EV charger design. This design incorporates a modified BL Landsman converter in tandem with a flyback converter, leveraging a Radial Basis Function Neural Network (RBFNN) for its control strategy. The

RBFNN control was specifically tailored to enhance the charger's operation in discontinuous conduction mode (DCM), showcasing a strategic reduction in the requirement for output sensors, thereby promising a leaner, cost-efficient solution. Simulation results vividly demonstrate the charger's capability to minimize input and output current ripples effectively, attributed to the intelligent modulation of the charging process by the RBFNN controller. Moreover, the simulated outcomes affirm the charger's compliance with the stringent IEC 61000-3-2 standard for power quality. These findings strongly position the proposed RBFNN-controlled BL converter-based charger as a highly efficient, cost-effective, and reliable alternative for advanced EV battery charging solutions, emphasizing significant advancements in power quality and factor improvement.

Conflict of interest statement

Authors declare that they do not have any conflict of interest.

REFERENCES

[1] S. Singh, S. Kewat, B. Singh, B. K. Panigrahi and M. K. Kushwaha, "Seamless Control of Solar PV Grid Interfaced System With Islanding Operation," in IEEE Power and Energy Technology Systems Journal, vol. 6, no. 3, pp. 162-171, 2019.

[2] A. K. Singh, S. Kumar and B. Singh, "Solar PV Energy Generation System Interfaced to Three Phase Grid With Improved Power Quality," in IEEE Transactions on Industrial Electronics, vol. 67, no. 5, pp. 3798-3808, 2020.

[3] A. I. Elsanabary, G. Konstantinou, S. Mekhilef, C. D. Townsend, M. Seyedmahmoudian and A. Stojcevski, "Medium Voltage Large-Scale Grid-Connected Photovoltaic Systems Using Cascaded H-Bridge and Modular Multilevel Converters: A Review," in IEEE Access, vol. 8, pp. 223686-223699, 2020.

[4] B. Zhu, G. Liu, Y. Zhang, Y. Huang and S. Hu, "Single-Switch High Step-Up Zeta Converter Based on Coat Circuit," in IEEE Access, vol. 9, pp. 5166-5176, 2021.

[5] Alzahrani, M. Ferdowsi and P. Shamsi, "A Family of Scalable Non-Isolated Interleaved DC-DC Boost Converters With Voltage Multiplier Cells," in IEEE Access, vol. 7, pp. 11707-11721, 2019.

[6] D. Bao, A. Kumar, X. Pan, X. Xiong, A. R. Beig and S. K. Singh, "Switched Inductor Double Switch High Gain DC-DC Converter for Renewable Applications," in IEEE Access, vol. 9, pp. 14259-14270, 2021.

[7] A. Ali et al., "Investigation of MPPT Techniques Under Uniform and Non-Uniform Solar Irradiation Condition–A Retrospection," in IEEE Access, vol. 8, pp. 127368-127392, 2020.

[8] L. Farah, A. Hussain, A. Kerrouche, C. Ieracitano, J. Ahmad and M. Mahmud, "A Highly-Efficient Fuzzy-Based Controller With High Reduction Inputs and Membership Functions for a Grid-Connected Photovoltaic System," in IEEE Access, vol. 8, pp. 163225-163237, 2020.

[9] M. Jedari Zare Zadeh and S. H. Fathi, "A New Approach for Photovoltaic Arrays Modeling and Maximum Power Point Estimation in Real Operating Conditions," in IEEE Transactions on Industrial Electronics, vol. 64, no. 12, pp. 9334-9343, 2017.

[10] M. N. H. Khan, M. Forouzesh, Y. P. Siwakoti, L. Li, T. Kerekes and F. Blaabjerg, "Transformerless Inverter Topologies for Single-Phase Photovoltaic Systems: A Comparative Review," in IEEE Journal of Emerging and Selected Topics in Power Electronics, vol. 8, no. 1, pp. 805-835, 2020.

[11] Y. Shan, J. Hu and J. M. Guerrero, "A Model Predictive Power Control Method for PV and Energy Storage Systems With Voltage Support Capability," in IEEE Transactions on Smart Grid, vol. 11, no. 2, pp. 1018-1029, 2020.

[12] C. Yanarates and Z. Zhou, "Symmetrical Pole Placement Method-Based Unity Proportional Gain Resonant and Gain Scheduled Proportional (PR-P) Controller With Harmonic Compensator for Single Phase Grid-Connected PV Inverters," in IEEE Access, vol. 9, pp. 93165-93181, 2021.

[13] R. Errouissi, A. Al-Durra and S. M. Muyeen, "Design and Implementation of a Nonlinear PI Predictive Controller for a Grid-Tied Photovoltaic Inverter," in IEEE Transactions on Industrial Electronics, vol. 64, no. 2, pp. 1241-1250, 2017.

[14] M. I. Mosaad, H. S. M. Ramadan, M. Aljohani, M. F. El-Naggar and S. S. M. Ghoneim, "Near-Optimal PI Controllers of STATCOM for Efficient Hybrid Renewable Power System," in IEEE Access, vol. 9, pp. 34119-34130, 2021.

[15] S. Yousaf, A. Mughees, M. G. Khan, A. A. Amin and M. Adnan, "A Comparative Analysis of Various Controller Techniques for Optimal Control of Smart Nano-Grid Using GA and PSO Algorithms," in IEEE Access, vol. 8, pp. 205696-205711, 2020.

[16] Limits for Harmonics Current Emissions (Equipment current per Phase), International standards IEC 61000-3-2, 2000. 16A

[17] Alessandro Malschitzky, Felipe Albuquerque, Eloi Agostini and Claudinor B. Nascimento, "Single-stage integrated bridgeless-boost nonresonant half-bridge converter for led driver applications," IEEE Transactions Industrial Electronics, vol. 65, no. 5, pp. 3866-3878, May 2018.

[18] Yeonho Jeong, Jae K. Kim and Gun W. Moon, "A bridgeless dual boost rectifier with soft-switching capability and minimized additional conduction loss," IEEE Transactions Industrial Electronics, vol. 65, no. 3, pp. 2226-2233, March 2018.

[19] Muntasir Alam, Wilson Eberle, Deepak S. Gautam, Chris Botting, Nicholas Dohmeier and Fariborz Musavi, "A hybrid resonant pulse-width modulation bridgeless AC–DC power factor correction converter," IEEE Transactions Industry Applications, vol. 53, no. 2, pp. 1406-1415, March-April 2017.

[20] Khairul S. B. Muhammad and Dylan D. C. Lu, "ZCS bridgeless boost PFC rectifier using only two active switches," IEEE Transactions Industrial Electronics, vol. 62, no. 5, pp. 2795-2806, May 2015.

[21] Julio C. Dias and Telles B. Lazzarin, "A family of voltage-multiplier unidirectional single-phase hybrid boost PFC rectifiers," IEEE Transactions Industrial Electronics, vol. 65, no. 1, pp. 232- 241, Jan. 2018.

[22] Ben Zhao, Alexander Abramovitz and Keyue Smedley, “Family of bridgeless buck-boost PFC rectifiers,” IEEE Transactions Power Electronics, vol. 30, no. 12, pp. 6524-6527, Dec. 2015.
[23] Vashist Bist and Bhim Singh, “An adjustable-speed PFC bridgeless buck–boost converter-fed BLDC motor drive,” IEEE Transactions Industrial Electronics, vol. 61, no. 6, pp. 2665-2677, June 2014.